Influence of irregular wave kinematics description on fatigue load analysis of offshore wind energy structures

K. Mittendorf[1], M. Kohlmeier[2], A. Habbar[2] and W. Zielke[2]

[1] Maritime Systems Engineering Department, Texas A&M at Galveston,
200 Seawolf Parkway, Galveston, Texas 77553, USA

[2] ForWind – Center for Wind Energy Research
Institute of Fluid Mechanics, University of Hannover,
Appelstr. 9a, 30167 Hannover, Germany

Abstract

For the optimization of offshore wind turbines, the fatigue design is of equal importance as the design against extreme events. Hence, the influence of directional irregular wave models on damage equivalent fatigue loads has been investigated. In most cases, real ocean waves differ significantly from the assumption of a linear superposition of unidirectional long crested individual waves with different heights and periods. The consideration of directional waves and the magnitude of spreading consequently affect the wave kinematics and therewith the wave loads; its extent is investigated in this contribution. Analyzed structures have been a monopile and a jacket construction (FINO platform), the simulation results have also been compared to strain measurements. The consideration of the waves' directionality results in an approximate reduction of the observed forces of up to 20% compared to unidirectional models.

1 Introduction

Concepts for highly optimized and robust offshore wind energy converters with a long lifespan are necessary to make offshore wind energy economically promising. Offshore wind parks are planned for different water depths. Dependent on the water depth, a variety of designs for the support structures of offshore wind energy converters are available. In moderate (or shallow) water depth gravity based foundations and monopile foundations have been used. For greater water depths tripod or jacket foundations seems to be feasible. In most cases, deep water ocean waves differ significantly from the assumption of a linear superposition of unidirectional long crested individual waves with different heights and periods and consequently this affects the wave kinematics and therewith the wave loads. In comparison with deep water waves, shallow water waves show a nonlinear behavior, which affects the wave kinematics, too. The wave crests become steeper and the troughs shallower.

In this paper the influence of waves' directionality in combination with linear and nonlinear irregular wave models on damage equivalent fatigue loads in time domain simulations has been investigated. Analyzed structures have been a monopile and a jacket construction (FINO platform). The simulation results for the jacket have also been compared to strain measurements.

2 Random Wave Simulation

Commonly, sea states are described in terms of a wave spectrum and the definition of an equivalent sea state in the time domain is possible from an inverse Fourier transform. In practice, it is necessary to use a discrete finite formulation, which can be interpreted as a superimposition of numerous linear waves (for velocity potential Φ as well as for the surface elevation η) with amplitudes and frequencies determined from the variance spectrum of water surface elevations and a random phase [1].

The velocity and acceleration field of the water particles can be derived directly from the potential Φ. The contribution of the high frequency components to the velocity is exaggerated by an increased vertical displacement. Velocities reach a maximum near the surface under the crest, so the application of linear superposition in this region leads to an overestimation. Beneath the mean water level, this approach is in agreement with laboratory data [2] and shows a reasonable agreement. To compensate the model inadequacies near the surface, several stretching methods have been suggested in literature. For the following investigations a first order stretching formula by Wheeler [3] has been used. In the first order stretching techniques the effective water depth is modified using the instantaneous wave-free surface in computing the decay function.

In most cases real ocean waves still differ significantly from the preceding model assumption of irregular and long crested sea states. To get a more realistic simulation of sea state conditions, it is necessary not only to superimpose waves with different frequencies, amplitudes and phases, but also waves travelling in different directions (Figure 1).

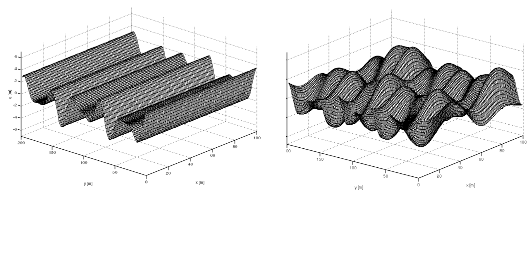

Figure 1 Unidirectional and directional irregular waves.

Forristall et al. [4] have observed considerable scatter between measured ocean wave velocities and the predictions of unidirectional theories with a clear bias toward over-prediction. Therefore the model of irregular ocean waves has been extended, so that the summation is made over frequencies and directions.

$$\phi(x,y,z,t) = \sum_i \sum_j a_{ij} \cdot \frac{g}{\omega_i} \cdot \frac{\cosh(k_i \cdot (h+z))}{\cosh(k_i \cdot h)} \cdot \sin(k_i \cdot \cos\theta_j \cdot x + k_i \cdot \sin\theta_j \cdot y - \omega_i \cdot t + \varepsilon_{ij})$$

$a_{ij}=(2 \cdot S(f,\theta) \cdot \Delta\omega_i \Delta\theta_j)^{0.5}$: wave amplitude
S(f,θ): directional wave spectrum
ω: angular wave frequency
ε: random phase
k: wave number
h: water depth
g: gravity
t: time
x,y,z: spatial coordinates

The directional spectrum S(f,θ) represents the distribution of wave energy in the frequency domain and its directional spreading. It is given by the product of the variance spectrum S(f) with a speading function D(f, θ). The directional function of the 2D-spectrum has influence on the wave crest length and with it on the structure of the sea surface. Variation of the speading function enables to simulate different sea state conditions like wind waves (Figure 2) or swell (Figure 3). Following, the $\cos^{2S}$-model by Mitsuyasu et al. [5] has been used.

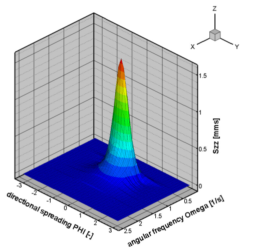

Figure 2 Directional spectrum (JONSWAP) for wind waves (H_s=7.0m, T_p=11.0s, spreading parameter S =10).

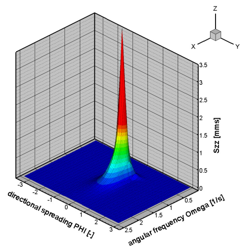

Figure 3 Directional spectrum (JONSWAP) for swell waves (H_s=7.0m, T_p=11.0s, spreading parameter S =75).

When waves travel from deep sea towards land they transform and get more non-linear. Troughs become wider and crests narrower and higher (Figure 4).

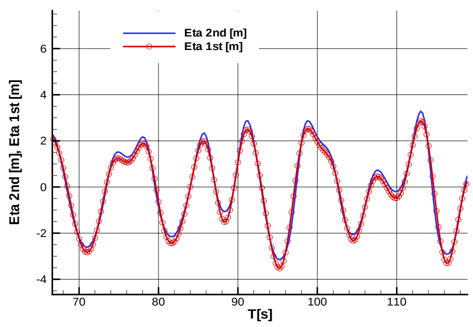

Figure 4 1st vs. 2nd order water surface elevation.

Methods for wave load simulation which are based on superposition of linear waves seem no longer reasonable, because linear wave theory has limited accuracy in these regions. Here, the nonlinear realization of waves has been made by pertubation method [6]. The velocity potential Φ is then represented in the following manner with the perturbation parameter absorbed into the function:

$$\phi(x,y,z,t) = \phi^{(1)}(x,y,z,t) + \phi^{(2)}(x,y,z,t) + ...$$

The performed calculations have been limited to second order accuracy.

3 Fatigue Analysis

The fatigue strength of the material has been represented by the S-N curves (Wöhler curves). The S-N curve gives the number of cycles N which a specimen can resist before breaking versus the stress range S. Usually the S-N curves are based on fatigue tests in the laboratory. Failure has occurred, when a crack has grown through the thickness of the component. Tests will be performed for different stress levels, the lower the stress range the larger the number of bearable cycles. This can be modelled by a simple double logarithmic equation:

$$N_{failure}(S) = \frac{S_1^m}{S^m} = \frac{K}{S^m}$$

S: stress range
S_1: fictive stress range, gives failure after one single cycle
$N_{failure}$: number of cycles to structure failure
m: slope of curve, material dependent
K: reference number of cycles

The stress ranges S are defined as a series of closed hysteresis loops in the stress cycles. For following analysis a modified rainflow counting introduced by Rychlik [7] has been used.
The fatigue damage has been calculated with the Palmgren-Miner rule, which is a linear damage accumulation hypothesis where the order of load events is not noticed.

$$D_{total} = \sum \frac{n(S_K)}{N_{failure}(S_K)}$$

S_k: k-th stress range
$n(S_k)$: actual number of cycles with stress range S_k
$N_{failure}(S_k)$: number of cycles to failure defined by S-N curve
D_{total}: accumulated damage

The estimation of the total damage or of the structure life time has been beyond the scope of this work. In fact, the goal has been to evaluate the effect of different random wave models on the fatigue damage. Thus, only the damage occurred in a single stationary sea state has been considered. The effect of different wave models has been compared in form of damage equivalent magnitudes (normal forces, moments and/or stress ranges). Damage equivalent magnitudes would lead to the same total damage for a given number of stress ranges n_E as the real observed stress collective. If the S-N curve is known, the damage equivalent stress range $\Delta\sigma_E$ (normal force ΔN or moment ΔM) (Figure 5) can be calculated as follows:

$$\Delta\sigma_E = \left(\frac{1}{n_E} \cdot \sum (\Delta\sigma_i^m \cdot n_i) \right)^{1/m}$$

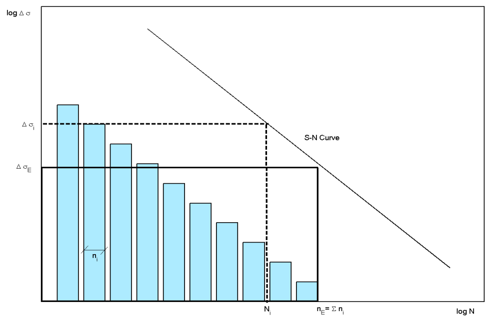

Figure 5 Damage equivalent stress range.

4 Distribution of Damage Equivalent Magnitudes for a Monopile in Random Sea

Three sets per 50 random realizations of response calculations have been made for a monopole structure with dimensions given in Figure 6.

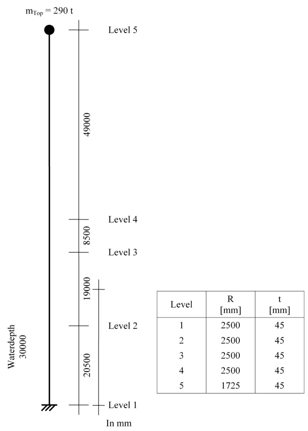

Figure 6 Monopile structure for analysis.

The calculations have been carried out with linear superposition model (directional and unidirectional) and the unidirectional second order random wave model, where the sea state has been described by a JONSWAP spectrum with significant wave height H_s= 7.46m and peak period T_p= 12.5s.
The influence of the different wave models on the fatigue load calculations has been studied for the moment M_y around the axis perpendicular to the wave propagation at mud level as well as for the horizontal reaction force F_x in wave direction. For a monopile structure this is believed to be clearly indicative of the differences in the effect of the use of different wave load models. In the directional case, the resulting reaction force or moment have been chosen for comparison with the unidirectional results. The resulting magnitudes have been determined by vector addition of the horizontal x- and y-components. The highest fatigue loads have resulted from the unidirectional 2^{nd} order model and the lowest from the directional 1^{st} order model. The difference in fatigue loads between 1D 2^{nd} order and 2D 1^{st} order random wave simulation is about 20%. The

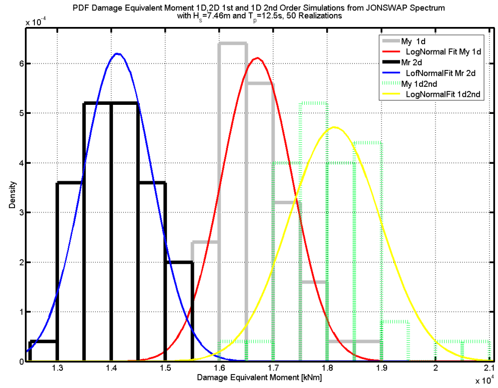

Figure 7 Empirical probability density function of damage equivalent moments, monopile.

empirical distributions of the resulting fatigue loads are given in Figure 7.
Moreover, the effect of variable wave spreading on the damage equivalent load has been investigated. Therefore, three sets of response calculations have been performed to simulate storm, swell and wind wave conditions. Within each set three different directional spreading parameter (S= 10, S= 25 and S= 75) have been used (Table 1).

Sea State	H_s	T_p	S
Storm	7.46m	12.5s	10, 25, 75
Wind waves	1.9m	5.9s	10, 25, 75
Swell	1.9m	8.3s	10, 25, 75

Table 1 Simulation parameters for variable spreading.

In case of a narrow banded spreading function (S= 75) the resulting damage equivalent fatigue loads have become highest and have been observed to be very close to the 1D result. A broadening of the directional spreading (S= 25 or S= 10) leads to a reduction in the total fatigue loads. The relative changes expressed by a normalization with the damage equivalent moment achieved in the simulation with spreading parameter S= 10 for the storm case are given in Figure 8. An increase in the spreading parameter results in a larger damage equivalent fatigue load**.**

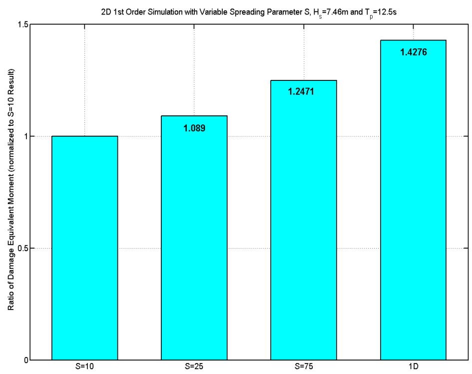

Figure 8 Ratio of damage equivalent moments at mud line (normalized) during storm conditions.

5 Comparison of Simulated and Measured Fatigue Loads for the FINO Platform

Measured strain time series from the research platform FINO1 (Figure 9) have been analyzed and compared to irregular random wave load simulations for different sea state conditions. Measured data are available for three positions (AVN, AVW and AVS) on level A of the platform close to the abutments and for three positions on a diagonal strut (DBDW, DBDSW and DBDS) on level B.

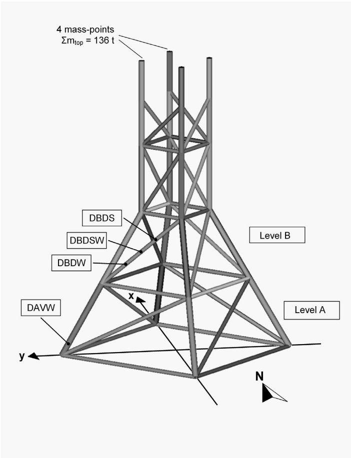

Figure 9 Simplified simulation model of the FINO platform.

The damage equivalent fatigue loads show a dependence on the sea state conditions, defined by significant wave height and peak period, as well as on the mean wave direction and the wave spreading [8]. The variation of the resulting fatigue loads for identical sea state parameters with changing mean direction (288º, 243º and 198º) is given in Figure 10. Differences in the total loads of more than 50% can be observed.

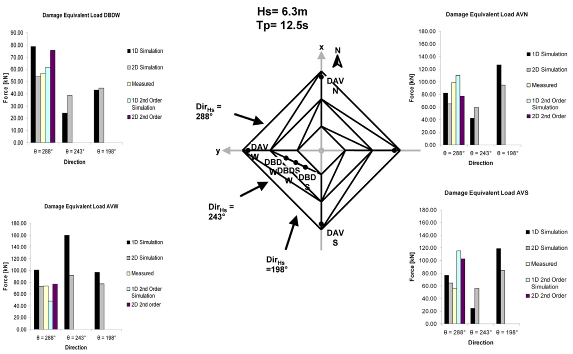

Figure 10 Measured and simulated damage equivalent fatigue loads of the FINO platform.

The simulated 1st order unidirectional fatigue loads have a clear trend to over predict the measured loads. The directional wave simulation approach with wave spreading has improved the results, but still shows smaller deviations in comparison with the measurements (Figure 10 and Figure 11).

6 Summary

The influence of different wave models on damage equivalent fatigue loads has been investigated. Simulation results have been compared to in-situ measurements. The largest damage equivalent fatigue loads have occurred in the 2nd order random wave simulation, followed by 1st order unidirectional, where a reduction of about 8% has been observed. A reduction of about 22% resulted by application of the 1st order directional random wave model. An investigation of the influence of the spreading leads to the conclusion, that a sea state with large spreading will produce smaller fatigue loads than a sea state with less spreading.

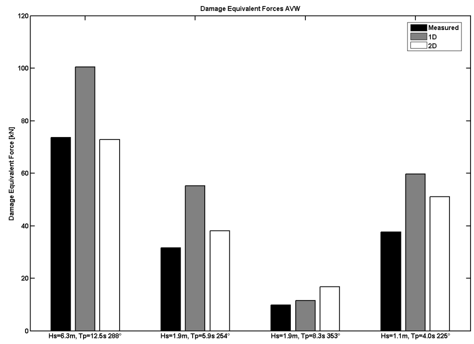

Figure 11 FINO, comparison of measured and simulated damage equivalent loads (position AVW) for different sea state conditions.

8 References

[1] Borgman, L. E. (1969). Ocean wave simulation for engineering design. J. of the Waterways and Harbors Division, 4:557 – 583.

[2] Dean, R. G. and Perlin, M. (1986). Intercomparison of near bottom kinematics by several wave theories and field and laboratory data. Coastal Engin., 9:399 - 437.

[3] Wheeler, J. (1970). Method for calculating forces produced by irregular waves. Journal of Petroleum Technology, pages 359 – 367.

[4] Forristall, G., Ward, E., Cardone, V. and Borgmann, L. (1978). The directional spectra and kinematics of surface gravity waves in tropical storm delia. Journ. of Physical Oceanography, 83:888 – 909.

[5] Mitsuyasu, H., Tasai, F., Suhara, T., Mizuno, S., Ohkusu, M., Honda, T., and Rikiishi, K. (1975). Observations of the directional spectrum of ocean waves using a cloverleaf buoy. J. of Physical Oceanography, 5:750 – 760.

[6] Sharma, J. and Dean, R. (1981). Second-order directional seas and associated wave forces. Society of Petroleum Engineers Jounral, 21:129 – 140.

[7] Rychlik, I. (1987). A new definition of the rainflow cycle counting method. Int. J. Fatigue, 9:119 – 121.

[8] Mittendorf, K. (2006). Hydromechanical Design Parameters and Design Loads for Offshore Wind Energy Converters, Doctoral Thesis, Institute of Fluid Mechanics, University of Hannover.